

PAPER

[View Article Online](#)
[View Journal](#) | [View Issue](#)

A thermodynamic gauge for mobile counter-ions from colloids and nanoparticles

Albert P. Philipse,* Bonny W. M. Kuipers and Agienus Vrij

Received 12th December 2014, Accepted 23rd December 2014

DOI: 10.1039/c4fd00261j

A thermodynamic equilibrium sensor is proposed that measures the ratio of the number of elementary charges z to the mass m of charged solutes such as charged colloids and nanoparticles. The sensor comprises a small, membrane-encapsulated salt solution volume that absorbs neutral salt molecules in response to the release of mobile counter-ions by charge carriers in the surrounding suspension. The sensor state emerges as a limiting case of the equilibrium salt imbalance, and the ensuing osmotic pressure difference, between arbitrary salt and suspension volumes. A weight concentration of charge carriers c is predicted to significantly increase the sensor's salt number density from its initial value $\rho_{s,0}$ to ρ_s^R , according to the relation $(\rho_s^R/\rho_{s,0})^2 - 1 = zc/m\rho_{s,0}$, under the assumption that the mobile ions involved in the thermodynamic sensor-suspension equilibrium are ideal and homogeneously distributed.

1. Introduction

Gradients in ion concentrations and osmotic pressure are inevitable phenomena for charged colloids^{1–3} and charged macromolecules that equilibrate slowly in comparison to their rapidly diffusing co- and counter-ions. The disparity in equilibration times often is imposed by an external, selective force such as gravity or a centrifugal force⁴ that primarily acts on the heavy carriers, or a semi-permeable membrane that only allows ions to permeate. Salt and osmotic pressure gradients are abundant phenomena in nature and technology; from the many biological examples, we mention the osmotic pressure difference between plant or animal cells and their surroundings, the regulation of which is essential for the cell's functioning.^{5,6} Regulation of the salt and osmotic pressure gradients of body fluids is also crucial for our health, with implications for numerous physiological and pathological phenomena, as extensively reviewed in ref. 7; osmometry is therefore a basic clinical tool in both human⁷ and

Van't Hoff Laboratory for Physical and Colloid Chemistry, Utrecht University, Debye Institute for Nano-materials Science, Padualaan 8, 3584 CH Utrecht, The Netherlands. E-mail: a.p.philipse@uu.nl

veterinary medicine.⁸ In membrane technology, osmotic pressure and salt gradients are encountered in the purification of electrolyte solutions *via* dialysis and, on a very large scale, in the desalination of sea water using reverse or forward osmosis.^{9,10}

Osmotic pressures and salt gradients^{11,12} have been studied *via* the classical Donnan equilibrium, recently reviewed in ref. 13, comprising a small volume of charge carriers in contact with an infinite electrolyte solution (the 'salt reservoir') which keeps the chemical potential of the salt at a constant value. However, in the majority of practical cases the reservoir is finite, such that its salt concentration adapts to the presence of charge carriers in the adjacent suspension. Typical examples of finite salt solutions are the biological cells mentioned above, the small supernatant volumes in contact with dense colloid sediments¹⁴ and the finite salt solution compartments in membrane osmometers.^{15,16} The variable salt concentration in a finite salt solution has, to our knowledge, not been investigated before, and the main motivation for this paper is to fill this gap in our understanding of the ionic equilibria associated with charged colloids and nanoparticles.

Instead of the usual infinite reservoir in the thermodynamics of charged species,^{1,3,13,20} we focus here on the opposite case of a salt solution that is very much smaller than the suspension of charge carriers. Such small solutions are of particular interest because their salt concentration responds to any mobile counter-ions that are released by charged solutes in their surroundings. In other words, a tiny salt solution may be employed as a sensor for the charge carried by solutes that cannot access the reservoir. The osmotic pressure difference between salt solution and surrounding suspension also contains information about the counter-ion concentration in a suspension. However, osmotic pressure determinations are often quite laborious; witness the extensive studies on magnetite nanoparticles^{17,18} and silica colloids.¹⁹ In addition, osmotic pressures depend on colloids as well as small ions. One advantage of a salt solution sensor is the absence of species other than small ions, so measurements of ion concentrations *via*, for example, spectroscopy or electrical resistance, are not disturbed by the presence of charge carriers.

In the thermodynamics of the sensor treated in this paper, essential parameters are the sensor's volume and salt concentration relative to the volume and salt concentration of the suspension. To develop a clear perspective on these parameters, we first analyze in Section 2 the equilibrium salt imbalance between arbitrary volumes of suspension and salt solution. Next we consider in Section 3, still for arbitrary volumes, the high-salt region where counter-ion densities are much smaller than reservoir salt concentrations. The limit of a large reservoir is the subject of Section 4, whereas the opposite case of a tiny salt solution is treated in Section 5. For the latter case we show how the solution's salt concentration monitors the density of mobile counter-ions in the suspension bulk. A salt imbalance entails an osmotic pressure difference between suspensions and salt solutions that is dealt with in Section 6. The Appendix documents the case of a membrane separating equal volumes of suspension and salt solution, a configuration that is relevant to consider as it also occurs in commercial osmometers.^{15,16}

2. Salt transfer from suspension to reservoir solution

In this section we analyze salt transfer from a suspension to arbitrary volumes of salt solution. Suspension and salt solution volumes are in all cases assumed to be electrically neutral, macroscopic volumes in which ideal ions experience only a constant electrical potential. Since ions diffuse in a zero-electric field, they are homogeneously distributed in both suspension and salt solution. It should be noted that this zero-field assumption, which considerably simplifies the calculation of the salt transfer, is realistic for sufficiently low charge densities on the charge carriers. This is shown, for example, for the case of interacting, parallel charged surfaces in ref. 3, where zero-field predictions are found to coincide with numerical solutions of the Poisson–Boltzmann equation for weakly charged surfaces.

2.1. The salt transfer equation

Consider a suspension volume V_i containing charge carriers such as colloids, proteins or poly-electrolytes, separated from a salt solution volume V_R by a membrane (Fig. 1), permeable only to solvent and small ions but impermeable to charge carriers. The initial state (Fig. 2) in the absence of charge carriers is a volume V_i that only contains salt such that in equilibrium the number density $\rho_{s,0}$ of salt molecules in the suspension equals that of the salt solution. Assuming a fully dissociated 1 : 1

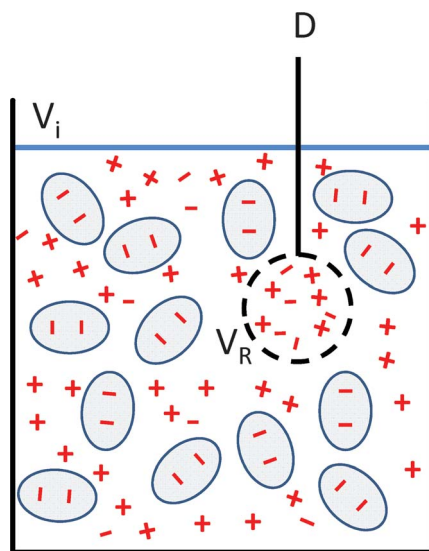


Fig. 1 A small salt solution volume V_R separated from a large suspension volume $V_i = \theta V_R$ with $\theta \gg 1$ by a membrane (dashed line) permeable only to solvent and ions but impermeable to charge carriers. The volume V_R adsorbs neutral salt molecules from the suspension in response to mobile counter-ions released by the charge carriers. Connected to some device D (for example, a conductivity meter) that measures the salt adsorption, the volume V_R acts as a sensor for the valency of the charge carriers, as further explained in Section 5.

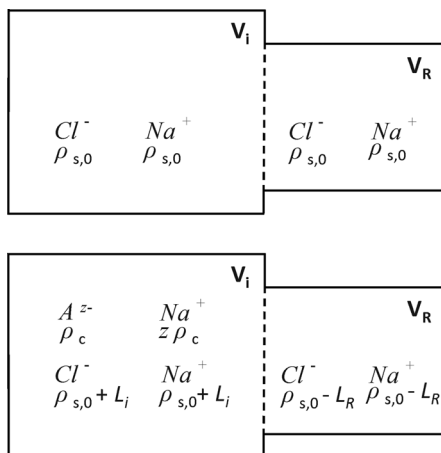


Fig. 2 Scheme for the derivation of salt transfer in Section 2.1. Top: initially the equilibrium salt concentration everywhere equals $\rho_{s,0}$. Bottom: when charge carriers with valency z are added to the suspension volume V_i , a counter-ion number density $z\rho_c$ is released, inducing an expulsion L_i of salt concentration to the salt solution volume V_R where the equilibrium salt concentration increases by an amount $-L_R$.

electrolyte such as NaCl, the total initial ion concentration then everywhere equals $2\rho_{s,0}$. The initial equilibrium state is perturbed (Fig. 2) by the addition of a number density ρ_c of charge carriers to the suspension volume, each carrier subsequently producing a large anion and z positive (sodium) counter-ions. The Na^+ concentration in the suspension now exceeds its equilibrium value and, consequently, sodium ions spontaneously migrate to the salt solution, accompanied by Cl^- anions to maintain overall electro-neutrality. When thermodynamic equilibrium has been restored, the anion density ρ_-^i in the suspension equals:

$$\rho_-^i = \rho_{s,0} + L_i; L_i < 0, \quad (1)$$

where L_i is the salt transfer to the salt solution which equals the decrease in the anion number density of the suspension; note that ρ_-^i equals the concentration of salt molecules in the suspension. The equilibrium cation density ρ_+^i in the suspension is given by (Fig. 2):

$$\rho_+^i = \rho_c z + \rho_-^i = \rho_c z + \rho_{s,0} + L_i, \quad (2)$$

where $\rho_c z$ is the number density of mobile counter-ions released by the charge carriers. The charge carriers are assumed to be strong electrolytes such that their valency z is constant; any charge regulation is disregarded here. The equilibrium number density of ions in the salt solution is:

$$\rho_-^R = \rho_+^R = \rho_s^R = \rho_{s,0} - L_R; L_R < 0. \quad (3)$$

Here, $-L_R$ is the increase in salt concentration due to salt molecules received from the suspension *via* the semi-permeable membrane. Since suspension *i* and

salt solution R jointly form a closed, isochoric system, salt is conserved such that the changes L_i and L_R in salt concentrations are coupled *via*:

$$L_R = \theta L_i; \quad \theta = \frac{V_i}{V_R}. \quad (4)$$

The parameter θ , an essential quantity in what follows, is the ratio of the suspension volume to the volume of the salt solution. The equilibrium salt concentrations in suspension and solution are denoted by, respectively, ρ_-^i and ρ_s^R ; the difference $\rho_-^i - \rho_s^R$ is the equilibrium salt imbalance. The latter should be distinguished from the salt transfer L_i , *i.e.* the salt concentration expelled by the suspension needed to establish the salt imbalance. The relation between salt transfer and salt imbalance is:

$$\rho_-^i - \rho_s^R = (\rho_{s,0} + L_i) - (\rho_{s,0} - L_R) = (1 + \theta)L_i = \left(\frac{1 + \theta}{\theta}\right)L_R, \quad (5)$$

here we have also made use of the salt conservation in eqn (4). Note that in (5), since $L_i < 0$, the salt concentration in the solution always exceeds the salt concentration of the suspension. We will now investigate how salt transfer L_i depends on the volume ratio θ in (4) and the ion densities in suspension and solution. The chemical potential of ideal cations and anions is given by:²⁰

$$\mu_{\pm} = \mu_{\pm,0} + kT \ln \left[\frac{\rho_{\pm}}{\rho_{\pm,0}} \right] \pm e\psi, \quad (6)$$

where $\mu_{\pm,0}$ is the standard chemical potential for a reference number density $\rho_{\pm,0}$, kT is the thermal energy, e is the proton charge and ψ is the constant electrical potential (also known as the Donnan potential¹³) in either suspension or salt solution. To maintain electro-neutrality, only pairs of anions and cations can migrate from suspension to salt solution or *vice versa*. The corresponding chemical potential of neutral salt molecules is $\mu_s = \mu_+ + \mu_-$,²⁰ such that the Donnan potential terms from (6) cancel:

$$\mu_s = \mu_{s,0} + kT \ln \left[\frac{\rho_+ \rho_-}{(\rho_{s,0})^2} \right]; \quad (\rho_{s,0})^2 = \rho_{+,0} \rho_{-,0}. \quad (7)$$

In equilibrium, the salt chemical potential in the solutions at both sides of the membrane in Fig. 1 and 2 must be equal. The substitution of (7) in the equilibrium condition $\mu_s^i = \mu_s^R$ yields:

$$\rho_+^i \rho_-^i = \rho_+^R \rho_-^R. \quad (8)$$

Substitution of eqn (1)–(4) in (8) modifies this equilibrium condition to:

$$(\rho_c z + \rho_{s,0} + L_i)(\rho_{s,0} + L_i) = (\rho_{s,0} - \theta L_i)^2, \quad (9)$$

from which we obtain the following quadratic for the salt concentration L_i expelled from suspension i to salt solution R:

$$(\theta^2 - 1) \left(\frac{L_i}{\rho_{s,0}} \right)^2 - 2(1 + \theta + y) \left(\frac{L_i}{\rho_{s,0}} \right) - 2y = 0; \quad y = \frac{z\rho_c}{2\rho_{s,0}} \quad \text{and} \quad \theta = \frac{V_i}{V_R}. \quad (10)$$

This quadratic shows that salt transfer from suspension to salt solution only depends on two dimensionless ratios, namely the volume ratio θ introduced in eqn (4) and the ratio y between the number density $z\rho_c$ of mobile counter-ions to the total ion number density $2\rho_{s,0}$ in the initial colloid-free salt solution. We will return to these ratios in later sections; here we continue with the two solutions of the quadratic (10):

$$(\theta^2 - 1) \frac{L_i}{\rho_{s,0}} = (1 + \theta + y) \pm \sqrt{(1 + \theta + y)^2 + 2(\theta^2 - 1)y}. \quad (11)$$

The physically correct solution from (11) follows from the requirement that $L_i < 0$: the suspension expels salt to the solution, not *vice versa*. This rules out the positive root in (11) which entails that $L_i > 0$ for volume ratios $\theta > 1$. The solution with the negative root can be rewritten as:

$$(\theta - 1) \frac{L_i}{\rho_{s,0}} = 1 + \left(\frac{y}{1 + \theta}\right) - \sqrt{1 + 2\theta\left(\frac{y}{1 + \theta}\right) + \left(\frac{y}{1 + \theta}\right)^2}, \quad (12)$$

which is a convenient form to address the various limiting cases in later sections. The salt concentration increase $-L_R$ in the salt solution directly follows from the substitution of (4) in (12). Both L_i and L_R are plotted in Fig. 3 and 4, and are further discussed in Sections 4 and 5. From measurements of salt concentrations in a reservoir with known volume, one can determine y and thus the particle charge – *via* a fit to eqn (12). In Section 5.2 we will examine the ‘sensor’ conditions under which the expression for L_R simplifies to a simple relation between L_R and y that is independent of the reservoir volume.

2.2. Limiting solution volumes and salt concentrations

With respect to the volume ratio θ introduced in (4), the two limiting cases of interest are the large-reservoir limit $\theta \ll 1$ and the small-solution limit $\theta \gg 1$; the intermediate case $\theta = 1$ of equal suspension and reservoir volumes is treated in the Appendix. The large-reservoir limit denotes a salt solution volume sufficiently large to maintain a constant salt concentration while the salt concentration of the suspension decreases; in the small-solution limit $\theta \gg 1$ it is the salt concentration of the suspension that remains constant while the salt concentration of the solution increases. The inequality $\theta \gg 1$ is of special interest here because a minute solution can be employed as an analytical tool for the charged solutes, as will become clear in Section 5. The large-reservoir limit $\theta \ll 1$ includes the asymptote $\theta \rightarrow 0$ because the salt solution can be arbitrarily large as in the case of a salt water ocean in which a suspension-filled dialysis bag is immersed. In the opposite sensor limit $\theta \gg 1$, however, the salt solution cannot be arbitrarily small because of the assumptions underlying salt transfer in eqn (12): the reservoir must remain a macroscopic, neutral volume with negligible fluctuations in ion densities.

One limiting case for concentrations of ions and colloids is the high-salt region, defined as the concentration domain where the following inequality is satisfied:

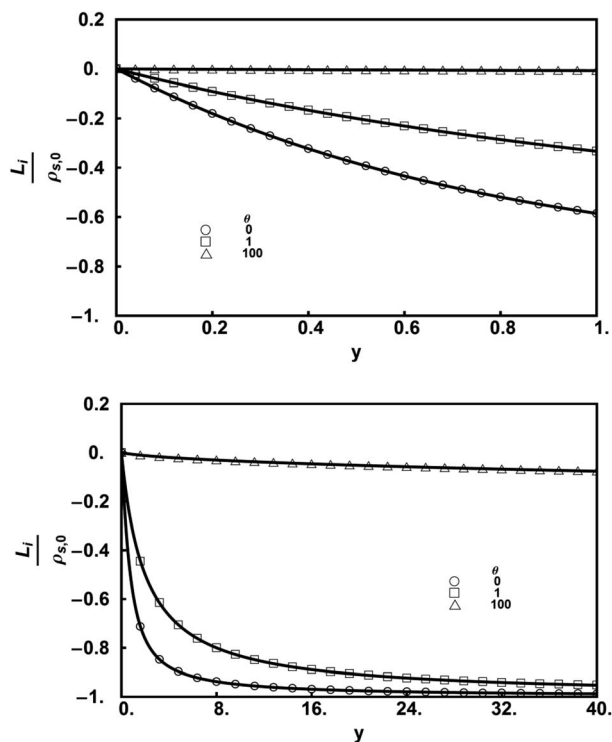


Fig. 3 A suspension volume V_i contains an initial salt number density $\rho_{s,0}$; after addition of a number density ρ_c of z -valent charge carriers, a salt concentration L_i is expelled to a salt solution with volume $V_R = V_i/\theta$. Shown here is L_i from eqn (12) versus the ion density ratio $y = z\rho_c/2\rho_{s,0}$ for various values of the volume ratio θ . In the high-salt region $y \ll 1$, L_i decreases linearly with y in accordance with eqn (18). The bottom figure shows that the low-salt region $L_i/\rho_{s,0} \approx -1$, where most of the initial salt has been expelled from the suspension, is only accessible for a large reservoir for which $0 \leq \theta < 1$.

$$y \ll 1 \Rightarrow z\rho_c \ll 2\rho_{s,0}; \quad y = \frac{z\rho_c}{2\rho_{s,0}}; \quad \theta \geq 0. \quad (13)$$

In words, in the high-salt region the initial salt concentration in solution and suspension volumes is much higher than the counter-ion densities released by charge carriers added to the suspension. As specified in (13) via $\theta \geq 0$, the high-salt region in the suspension occurs for any solution volume, as will be demonstrated in Section 3. In addition to their common high-salt region, large and small salt solutions also have their own distinct salt-region. Only large reservoirs can enter the low-salt region where the reservoir has absorbed most of the suspension's salt such that counter-ions are the dominating ions in the suspension. This 'desalination' of a suspension cannot be achieved by solutions that are smaller than the suspension volume; the low-salt region is accordingly defined as:

$$y \gg 1 \text{ and } 0 \leq \theta < 1; \quad \theta = \frac{V_i}{V_R}. \quad (14)$$

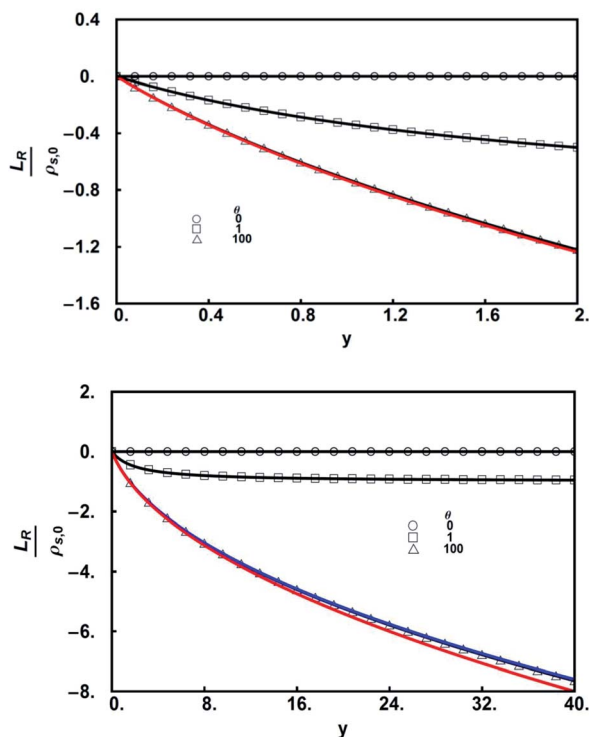


Fig. 4 Salt concentration increase in a reservoir, $-L_R$ from eqn (4) and (12), versus ion density ratio $y = z\rho_c/2\rho_{s,0}$ for three volume ratios θ . The square-root dependence $L_R/\rho_{s,0} = 1 - \sqrt{1+2y}$ from eqn (28) (solid red line) is valid for $\theta \gg 1$ and $y \ll \theta$, such that for a tiny sensor ($\theta \gg 1$) eqn (28) is applicable to fairly high y -values. Addition of the first correction term y/θ in (27) leads for $\theta = 100$ to the solid blue line: a perfect match to $-L_R$ from eqn (4) and (12) up to $y = 40$. Note that even in the high-salt region $y < 1$, the sensor picks up significant salt concentrations allowing, in principle, an accurate charge determination at even quite low colloid densities.

The distinguishing salt region in the small-reservoir limit is the sensor-salt region where the following inequalities are valid:

$$y \ll \theta \text{ and } \theta \gg 1. \quad (15)$$

In the sensor-salt region the salt concentration increase L_R in the small solution is independent of the solution volume, such that L_R depends only on the ion density ratio y , as further explained in Section 5.2.

3. Arbitrary reservoir volumes $\theta \geq 0$ in the high-salt region $y \ll 1$

One interesting feature of the high-salt region is that the salt transfer L_i from suspension to solution is described by an expansion of (12) that is valid for any solution volume. This results from the expansion of the square-root term in (12) for the high-salt inequality $y \ll 1$:

$$\sqrt{1 + 2\theta\left(\frac{y}{1+\theta}\right) + \left(\frac{y}{1+\theta}\right)^2} = 1 + \theta\left(\frac{y}{1+\theta}\right) + \frac{1}{2}(1-\theta^2)\left(\frac{y}{1+\theta}\right)^2 + \dots, \quad (16)$$

for $y \ll 1$.

Since the term $2\theta y/(1+\theta)$ is bound by:

$$0 \leq 2\theta\left(\frac{y}{1+\theta}\right) \leq 2y, \quad \text{for } \theta \geq 0, \quad (17)$$

it follows that for $y \ll 1$, the small-parameter expansion in (16) is applicable for any value of θ ; that is to say, the high-salt expansion (16) holds for arbitrary solution volumes. The substitution of (16) in (12) yields for the salt transfer from suspension to solution in the high-salt limit:

$$(1+\theta)\frac{L_i}{\rho_{s,0}} = -y + \frac{1}{2}y^2 + \dots, \quad \text{for } y \ll 1; \quad \theta \geq 0. \quad (18)$$

Eqn (18) describes a small perturbation of the initial salt concentration $\rho_{s,0}$ by the addition of small numbers of (weakly) charged colloids. Though $y \ll 1$, in (18) we have included the quadratic y^2 because it is this term that yields the first non-zero contribution to the osmotic pressure in the high-salt limit, as further discussed in Section 5. Omitting this quadratic, we find that on substitution of $L_i = \rho_-^i - \rho_{s,0}$ in (18):

$$\rho_-^i = \rho_{s,0} - \frac{z\rho_c}{2(1+\theta)}, \quad \text{for } y \ll 1; \quad \theta \geq 0. \quad (19)$$

This interesting result shows that in the high-salt concentration domain a fraction $1/2(1+\theta)$ of the number density $z\rho_c$ of mobile counter-ions is expelled to the salt solution *via* neutral salt molecules. The maximal fraction $1/2$ occurs for salt transfer to a large reservoir ($\theta \ll 1$), whereas in the small-solution limit $\theta \gg 1$ salt expulsion vanishes for the obvious reason that a tiny reservoir cannot desalinate a large suspension volume.

4. The large-reservoir limit $\theta \ll 1$

4.1. Arbitrary salt concentration $y \geq 0$

In an infinite reservoir the salt concentration remains constant, as indeed follows from the substitution of $\theta = 0$ in the salt conservation (4):

$$\frac{L_R}{\rho_{s,0}} = 0, \quad \text{for } \theta \rightarrow 0. \quad (20)$$

For the suspension, however, the absorption remains finite; from the salt transfer eqn (12) we find that in the large-reservoir limit $\theta \rightarrow 0$:

$$\frac{L_i}{\rho_{s,0}} = -y + \sqrt{1+y^2} - 1, \quad \text{for } \theta \rightarrow 0. \quad (21)$$

This result has also been derived in ref. 13, where more discussion can be found on this salt expulsion to an infinite reservoir. Note that since $L_i = \rho_-^i - \rho_{s,0}$, the salt concentration ρ_-^i in the suspension is:

$$\frac{\rho_-^i}{\rho_{s,0}} = \sqrt{1 + y^2} - y, \text{ for } \theta \rightarrow 0. \quad (22)$$

For $y > 0$, the RHS of (22) is always smaller than unity, which means that charged colloids always decrease the salt concentration in the suspension by salt expulsion to a large reservoir.

4.2. High- and low-salt regions

From the salt transfer eqn (21) we can infer that in the high-salt region, $y \ll 1$, the addition of charged colloids leads only to the small salt expulsion given by:

$$\frac{L_i}{\rho_{s,0}} = -y \Rightarrow \rho_-^i = \rho_{s,0} - \frac{1}{2} \rho_c z, \text{ for } \theta \rightarrow 0 \text{ and } y \ll 1, \quad (23)$$

as also follows from the general result (19). On entering the low-salt region the colloids expel significant salt concentrations to the large reservoir; for $y \gg 1$ the salt-transfer from eqn (21) approaches:

$$\frac{L_i}{\rho_{s,0}} = y \left[\left(1 + \frac{1}{2y^2} \right) - 1 \right] - 1 \sim \frac{1}{2y} - 1, \text{ for } \theta \rightarrow 0 \text{ and } y \gg 1. \quad (24)$$

Fig. 3 illustrates that for the large reservoir $\theta \rightarrow 0$, (24) is already a good approximation for the salt transfer to the reservoir at moderate y -values. For example, (24) yields $L_i/\rho_{s,0} = -0.875$ for $y = 4$, which is quite close to the salt expulsion obtained from the full eqn (12) (see the curve for $\theta = 0$ in the lower part of Fig. 3). Even for $y = 1$, the value $L_i/\rho_{s,0} = -0.5$ from (24) is near the value from eqn (12), as can be seen for the curve $\theta = 0$ in the upper part of Fig. 3. For small salt solutions, however, the low-salt region is out of reach. In Fig. 3 we can observe that already for $\theta = 1$, *i.e.* for a reservoir as large as the suspension, unrealistically large y -values are needed for the suspension to enter the low-salt region. This underlines the statement made in Section 2.2 that the low-salt region is distinctive for the large-reservoir limit. Note from (24) that in the low-salt region the salt concentration expelled by the suspension to reservoir asymptotes to $L_i \rightarrow -\rho_{s,0}$, which in view of the definition of L_i in eqn (1) is equivalent to $\rho_-^i \rightarrow 0$: the limit in which all anions have left the suspension.

5. The small-solution limit $\theta \gg 1$

5.1. Arbitrary salt concentration $y \geq 0$

In the limit $\theta \gg 1$ for a tiny solution the negative salt adsorption L_i of the suspension in (12) asymptotes to:

$$\frac{L_i}{\rho_{s,0}} = 0, \Rightarrow \rho_-^i = \rho_{s,0}; \text{ for } \theta \gg 1. \quad (25)$$

The outcome in (25) is clear: the salt concentration in the suspension volume hardly changes when the suspension can only expel a small amount of salt to a tiny solution; see also the curve for $\theta = 100$ in Fig. 3. However, in contrast to the salt expulsion L_i from the bulk suspension in (25), the salt adsorption L_R by the tiny salt solution is quite substantial. For $\theta \gg 1$, we find from (4) and (12) the general result for the salt concentration rise in a tiny solution:

$$\frac{L_R}{\rho_{s,0}} = 1 + \frac{y}{\theta} - \sqrt{1 + 2y + \left(\frac{y}{\theta}\right)^2}, \text{ for } \theta \gg 1 \text{ and } y \geq 0. \quad (26)$$

Here we have made explicit *via* $y \geq 0$ that the salt concentration increase in the small solution according to (26) is still valid for any value of the ion density ratio y .

5.2. Sensor-salt region $y \ll \theta$

Next we narrow down the domain of y to the region where the ion density ratio y is smaller than the volume ratio θ ; for this region (26) becomes:

$$\frac{L_R}{\rho_{s,0}} = 1 + \frac{y}{\theta} - \sqrt{1 + 2y}, \text{ for } \theta \gg 1 \text{ and } 0 \leq y \leq \theta. \quad (27)$$

Fig. 4 shows that (27) is a very accurate approximation for the salt concentration increase L_R in a small solution, up to the maximal ion density ratio $y = 40$ in the lower part of the figure. The solid blue line in Fig. 4 also illustrates that the dependence in (27) on the small solution volume *via* the term y/θ represents only a minor correction on the salt concentration increase L_R , which can be omitted when we further restrict the y -region by imposing the inequality $y \ll \theta$:

$$\frac{L_R}{\rho_{s,0}} = 1 - \sqrt{1 + 2y}, \text{ for } \theta \gg 1 \text{ and } 0 \leq y \ll \theta. \quad (28)$$

We will use the term ‘sensor-salt region’ for the ion density range $y \ll \theta$: it is in this region that the salt uptake by the small solution acts as a sensor, meaning that the salt uptake stands in a simple relation to y that is independent of the solution volume. The usage of (28) to determine the number of mobile counterions, z , released by a colloid is further examined in Section 7. Note that the sensor-salt region includes the high-salt case $y \ll 1$, where L_R from (28) further simplifies to:

$$\frac{L_R}{\rho_{s,0}} = -y + \frac{1}{2}y^2 + \dots \sim -y, \text{ for } \theta \gg 1 \text{ and } 0 \leq y \ll 1. \quad (29)$$

This is an instance of the high-salt region already encountered in eqn (18); substitution of $(1 + \theta)L_i \approx \theta L_i = L_R$ in eqn (18) indeed yields (29). It is important to note that eqn (28) spans quite a wide range of y -values since the volume ratio in an experimental set-up¹¹ may be as large as $\theta \sim 1000$, so the inequality $y \ll \theta$ will easily be satisfied. The wide y -validity range is further illustrated by Fig. 4, which shows the salt concentration increase in the reservoir according to eqn (4) and (12) as function of y . For a small reservoir with $\theta = 100$, one observes that eqn (28),

plotted as the red line in Fig. 4, is very accurate up to $y \approx 10$, and still a reasonably good approximation even up to $y \approx 15$; thus a wide range of colloid concentrations can in principle be accessed.

6. Osmotic pressure differences between suspensions and reservoir

6.1. Arbitrary reservoir volumes $\theta \geq 0$

The salt migration quantified by eqn (12) also determines the excess osmotic pressure of the suspension relative to the salt solution. To derive this excess osmotic pressure Π we start with the Donnan equation of state, reviewed in ref. 13:

$$\frac{\Pi}{kT} = \frac{\Pi(y=0)}{kT} + \rho_-^i + \rho_+^i - 2\rho_s^R, \quad (30)$$

where $\Pi(y=0)$ is the osmotic pressure exerted by the charge carriers in their uncharged state, supplemented by the pressure due to excess ions in the suspension. Incidentally, the contribution $\Pi(y=0)$ does not assume that the carriers are ideal: their shape, size and concentration are arbitrary, as derived and discussed in detail in ref. 13. The assumptions underlying (30) are that ions are ideal and homogeneously distributed,¹³ the same assumptions that are also employed in Section 2: osmotic pressure and salt imbalance are treated here on exactly the same level of approximation. On substitution of eqn (1)–(4) in the Donnan osmotic pressure (30) we obtain:

$$\frac{\Pi - \Pi(y=0)}{2\rho_{s,0}kT} = y + (1 + \theta) \frac{L_i}{\rho_{s,0}}; \quad \theta = \frac{V_i}{V_R}; \quad y = \frac{\rho_c z}{2\rho_{s,0}}. \quad (31)$$

Here, pressures are rescaled on the osmotic pressure $2\rho_{s,0}kT$ of the initial colloid-free salt solution. The osmotic pressure in the form of (31) clearly illustrates its physical basis: when the carriers are uncharged, both y and L_i in (31) are zero, such that $\Pi = \Pi(y=0)$. When the carriers with number density ρ_c are charged to a valency z , the maximal pressure rise due to released counter-ions is $\Pi - \Pi(y=0) = z\rho_c kT$. However, the pressure difference across the membrane is diminished by $L_i < 0$ in (31) due to the migration of salt from the suspension to the salt solution.

6.2. Arbitrary reservoir volumes $\theta \geq 0$ in the high-salt region $y \ll 1$

The osmotic pressure drop across the membrane between suspension and solution when the suspension is in the high-salt region follows from the substitution of salt transfer eqn (18) in (31):

$$\frac{\Pi - \Pi(y=0)}{2\rho_{s,0}kT} = \frac{1}{2}y^2, \quad \text{for } y \ll 1; \quad \theta \geq 0. \quad (32)$$

Thus the excess osmotic pressure of the suspension is a quadratic that is independent of the solution volume. Eqn (32) can be rewritten as:

$$\frac{\Pi - \Pi(y=0)}{kT} = \left(\frac{z^2}{4\rho_{s,0}} \right) \rho_c^2, \text{ for } y \ll 1; \theta \geq 0. \quad (33)$$

This quadratic in the colloid density represents the first-order correction to the osmotic pressure of uncharged colloids relative to the reservoir. Previously this quadratic has only been derived for colloids in a suspension that is connected to an infinite salt reservoir;¹³ we find here that this first-order correction is actually independent of the reservoir size. Fig. 5 (top) clearly illustrates this independence: when plotted against y^2 , osmotic pressures merge to one linear curve on approach of the uncharged colloids at $y = 0$.

6.3. The large-reservoir limit $\theta \ll 1$

The osmotic pressure difference between a small suspension volume and a large salt reservoir is part of the classical Donnan equilibrium reviewed in ref. 13; here we briefly recapitulate some results, also for comparison to the pressure exerted on a sensor in Section 6.4. The osmotic pressure difference between a small

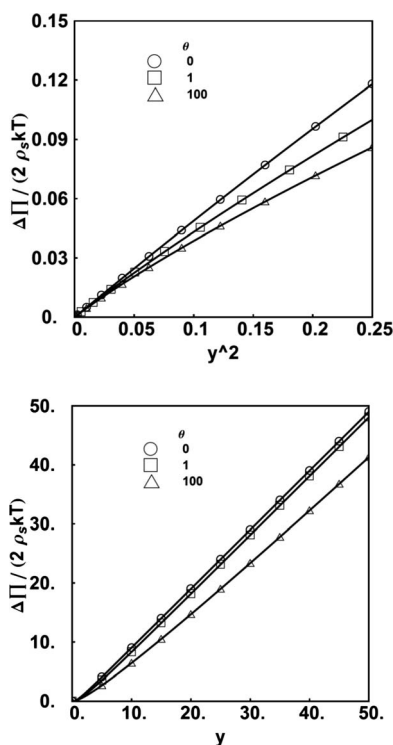


Fig. 5 Top: osmotic pressure difference from (31) versus the square of the ion density ratio y , for various volume ratios θ . In the high-salt domain $y \ll 1$, the pressure increases as $(1/2) y^2$, independent of the salt solution volume, in accordance with (32). Bottom: only large reservoirs access the low-salt region where the pressure increases linearly with y ; for small solution volumes ($\theta \gg 1$) this low-salt region is out of reach, as shown here for the case $\theta = 100$. Note that reducing the reservoir size for a given value of y also reduces the osmotic pressure drop across the membrane between the suspension and salt solution.

suspension volume and a large salt reservoir readily follows from the substitution of (21) in (31):

$$\frac{\Pi - \Pi(y=0)}{2\rho_{s,0}kT} = \sqrt{1+y^2} - 1, \text{ for } \theta \rightarrow 0, \quad (34)$$

which indeed equals the Donnan osmotic pressure difference between a suspension and an infinite salt reservoir, as derived in ref. 13. The low-salt region $y \gg 1$ follows from the substitution of the salt transfer ($L_i/\rho_{s,0}$) from eqn (24) in (31):

$$\frac{\Pi - \Pi(y=0)}{2\rho_{s,0}kT} = y + \frac{1}{2y} - 1 \sim y, \text{ for } y \gg 1 \text{ and } \theta \ll 1. \quad (35)$$

Eqn (35) confirms that in the low-salt region the pressure difference across the membrane is dominated by the counter-ions *via* the linear y -term. As noted earlier, a suspension can only access the low-salt domain when connected to an electrolyte reservoir of larger volume. In Fig. 5, one indeed observes that the excess osmotic suspension pressure for an infinite reservoir ($\theta \rightarrow 0$) easily reaches the no-salt region, where the pressure increases linearly with y according to (35). However, for a small solution with $\theta = 100$ (open triangles in Fig. 5), the pressure remains below the no-salt limit, even for the largest y -value: the suspension is unable to expel all co-ions to the small solution.

6.4. The small-solution limit $\theta \gg 1$

The osmotic pressure exerted by a bulk suspension on a small salt solution follows from (31) and the salt conservation in (4):

$$\frac{\Pi - \Pi(y=0)}{2\rho_{s,0}kT} = y + \frac{L_R}{\rho_{s,0}} \frac{1+\theta}{\theta} = y + \frac{L_R}{\rho_{s,0}}; \text{ for } \theta \gg 1. \quad (36)$$

Substitution of the salt absorption L_R of the small sensor from eqn (28) in (36) yields:

$$\frac{\Pi - \Pi(y=0)}{2\rho_{s,0}kT} = 1 + y - \sqrt{1+2y}, \text{ for } \theta \gg 1 \text{ and } y \ll \theta. \quad (37)$$

On comparison of this pressure exerted on a small solution volume to the excess osmotic pressure (34) applied by a suspension on a large reservoir, a comparison also made in Fig. 5, we notice that in the high-salt region $y \ll 1$, both pressures are the same. However, outside the high-salt region, the pressure exerted on the sensor is always smaller than that applied by the same suspension on a large reservoir. This mitigation of the pressure on the sensor is apparently due to the rise of the sensor's salt concentration, which diminishes the salt imbalance between suspension and solution.

7. Discussion

The main result from the analysis in Section 2 is the general expression (12) for salt transfer from a suspension to a salt solution; general in the sense that it holds

for arbitrary salt and suspension volumes and that it is a rigorous consequence of the assumptions that salt is in equilibrium according to eqn (8) and conserved according to eqn (4).

Fig. 3 illustrates that for a small reservoir ($\theta = 100$), the salt concentration in the suspension remains virtually constant, and that for a given value of the colloid concentration, *i.e.* a given value of y , the suspension is able to expel more salt when the salt solution volume increases (see the curves for $\theta = 1$ and $\theta = 0$ in Fig. 3). Fig. 4 shows that the equilibrium salt concentration in an infinite reservoir remains constant, as could be expected. For decreasing salt solution volumes at a given value of y , the solution absorbs an increasing salt concentration. Note in Fig. 4 that for a small salt solution with $\theta = 100$ (in practice¹¹ one easily realizes $\theta \approx 1000$), the salt concentration increase in the sensor is considerable, even at small y -values. This is important for the utilization of a small salt solution volume as a charge sensor, as further discussed below.

In the analysis of the salt equilibrium between the suspension and salt solution, we have employed a semi-permeable membrane, as indicated in Fig. 1 and 2. From a thermodynamic viewpoint such a membrane is not necessary:¹³ the sole requirement is that ions equilibrate fast on the time scale of the much slower colloids. It does not matter what makes the colloids slow: their large size, an external field such as gravity,⁴ or a restriction in the form of a membrane. However, for the case of a suspension in contact with a small volume of salt solution, the required separation of time scales for colloids and ions becomes problematic as the small solution will be quickly infiltrated by diffusing colloids unless, indeed, a membrane prevents this colloid infusion.

From measurements of the salt concentration increase L_R in a solution with known volume ratio θ , one could determine $y = z\rho_c/2\rho_{s,0}$ and thus the particle charge z *via* a fit to L_R from eqn (4) and (12). This fit is valid for any value of y , as long as the ions are ideal and homogeneously distributed, as is assumed in the derivation of (12). In Section 5.2 we found that for small solutions $\theta \gg 1$ in the sensor-salt region $y \ll \theta$ eqn (28) is valid; its implication is that the salt concentration increase L_R only depends on the number z of mobile counter-ions released per charge carrier, provided, of course, the colloid concentration is known. The experimental concentration measure is the colloid weight concentration c , so it is convenient to rewrite (28) as:

$$\frac{\rho_s^R}{\rho_{s,0}} = \sqrt{1 + \frac{z}{m} \frac{c}{\rho_{s,0}}}, \text{ for } \theta \gg 1 \text{ and } y \ll \theta, \quad (38)$$

where m is the mass of the charge carriers. The high-salt limit of (38) is:

$$\frac{\rho_s^R}{\rho_{s,0}} = 1 + \frac{z}{2m} \frac{c}{\rho_{s,0}}, \text{ for } \theta \gg 1 \text{ and } y \ll 1. \quad (39)$$

We can see in (38) and (39) that the salt concentration ρ_s^R in the sensor actually probes the charge-to-mass ratio of the charged species that cannot permeate the membrane separating the sensor from the adjacent suspension. Note that $z/2m$ is the initial slope in the salt concentration of the sensor *versus* the weight concentration of added colloids; in the limit $c \rightarrow 0$ salt always dominates the counter-ions.

The square-root dependence of the salt concentration of the sensor on the ion ratio y in eqn (38) is expected to be valid for a substantial range of values of y , as we already noted in the discussion of Fig. 4. Thus for a small sensor, the fit to (38) is predicted to apply up to fairly high colloid concentrations – at least as long as the assumption of homogeneously distributed, ideal ions remains valid. Several other interesting features of sensors based on eqn (38) are the following. First, (38) is independent of θ : the sensor's volume is irrelevant as long as the volume is small in comparison to the suspension volume. Secondly, the charge-to-mass ratio z/m is the only unknown, and only the salt concentration change L_R of the sensor needs to be measured, which can be done accurately *via* the sensor's electrical conductivity. A third point to notice with respect to eqn (38) is that the species carrying the fixed surface charge are not restricted to solid colloids: poly-electrolytes and proteins (in short any charge carrier that cannot permeate the membrane) can also be the charge carrier here. In addition, their shape and concentration are also irrelevant because they only affect in eqn (31) the reference pressure $\Pi(y = 0)$ of uncharged colloids. Thus the sensor could also be used to probe the charge-to-mass ratio of, for example, a poly-electrolyte gel or a network of flocculated colloids.

Osmotic pressure differences between suspensions and salt solutions can also be utilized to determine the ion density ratio y and therefore the particle charge;^{4,19} one could employ the pressure difference (34) between a suspension and a large reservoir or the osmotic pressure difference (37) between a suspension and a sensor. The latter, incidentally, is smaller than the pressure difference between a suspension and a large reservoir (see also Fig. 5), except in the high-salt region where the pressure is the same quadratic (32) for all reservoir volumes. One disadvantage of osmometry in comparison to a sensor is the colloid contribution to the osmotic pressure, whereas measurements of salt concentrations in sensors are not affected by the presence of any species other than small ions. This difference between osmometry and charge sensors, it should be noted, is an experimental one – the thermodynamics underlying both methods is the same. The thermodynamic connection between salt imbalance and an osmotic pressure difference, here embodied by eqn (31), is further examined elsewhere.¹³ This thermodynamic basis makes charge determination *via* the sensor (and osmometry) in principle more straightforward than the usual kinetic electrophoresis methods which are quite involved in practice as well as in theory^{21,22} and which, in addition, are quite restricted with respect to colloid shape and concentration.

8. Conclusions and outlook

We have analyzed the thermodynamic equilibrium between a suspension of charge carriers such as charged colloids or nanoparticles, and a salt solution, both containing ideal, homogeneously distributed ions. The osmotic pressure difference between a suspension and salt solution is shown to be independent of the solution volume in the high-salt domain where salt dominates counter-ions. In the limit $\theta \rightarrow 0$ for an infinite reservoir, we recover known results from the Donnan equilibrium.¹³ For the opposite case $\theta \gg 1$, however, we find a new result: a minute region of salt solution that acts as a charge sensor for the charge carriers in the suspension bulk. The salt concentration of the sensor is linked to the ion density ratio y *via* the square-root dependence in eqn (38), which is

predicted to hold even for fairly high colloid concentrations, provided the assumption of homogeneously distributed, ideal ions remains valid.

The analysis in this paper applies to charge carriers with a constant number of surface charges. In addition, the carrier volume fraction in the suspension volume V_i is small, such that V_i approximately equals the available free volume for ions. Extension of the salt sensor to concentrated suspensions of carriers with regulated surface charge will be the subject of a future paper. The assumption that ions are ideal and homogeneously distributed will break down at sufficiently high ion densities and sufficiently high charge number densities on the carriers. To assess the validity range of results in this paper, computer simulations as for poly-electrolytes in ref. 23 would be very helpful to include the effects of ion correlations and electrical double-layers surrounding the charge carriers. Experiments are in progress to test eqn (38) using a charge sensor monitoring salt increase in time *via* the sensor's electrical impedance.¹¹ One system under investigation is an aqueous dispersion of charged silica nanoparticles.¹¹ For apolar fluids it would be interesting to investigate PbSe quantum dots that are suspected to carry charge in decalin,²⁴ though changes in resistivity might be too small here for a reliable gauge of mobile counter-ions.

Appendix

A Equal suspension and salt volumes ($\theta = 1$)

In the main text we have analyzed salt transfer to arbitrary salt solution volumes ($\theta \geq 0$), and considered the specific cases of an infinite reservoir and a very small solution. Here we will document the case of equal salt and suspension volumes; this is practically relevant as commercial osmometers are available^{15,16} where volumes at both sides of the membrane are indeed of comparable magnitude. To find the salt transfer for the case $\theta = 1$, consider a small deviation ε from $\theta = 1$:

$$\theta = 1 + \varepsilon; 0 \leq |\varepsilon| \ll 1. \quad (40)$$

Substitution of (40) in (12) yields:

$$2\varepsilon \frac{L_i}{\rho_{s,0}} = (2+y) \left[1 - \sqrt{1 + \frac{4\varepsilon y}{(2+y)^2}} \right] \text{ for } \varepsilon \ll 1, \quad (41)$$

which upon linearization of the square-root leads to the salt expulsion to an equal-sized reservoir:

$$\frac{L_i}{\rho_{s,0}} = \frac{-y}{y+2}, \text{ for } \theta = 1. \quad (42)$$

Fig. 3 illustrates that the case $\theta = 1$ already represents a significant decrease in the salt expulsion in comparison to the large reservoir $\theta = 0$: finite reservoir size in an osmometer cannot be ignored. When mobile counter-ions from the colloids in the suspension outnumber salt ions such that $y \gg 1$, eqn (42) approaches:

$$\frac{L_i}{\rho_{s,0}} = -1 + \frac{2}{y} + \dots \sim -1, \text{ for } \theta = 1 \text{ and } y \gg 1, \quad (43)$$

which asymptotes to $L_i = -\rho_{s,0}$, i.e. the limit in which the suspension has expelled all its salt to a reservoir of equal size. On the other hand, for the high-salt inequality $y \ll 1$, eqn (42) yields:

$$\frac{L_i}{\rho_{s,0}} = -\frac{1}{2}y + \frac{1}{4}y^2 + \dots \text{ for } \theta = 1 \text{ and } y \ll 1, \quad (44)$$

in accordance with (18). From the leading term we find:

$$\frac{L_i}{\rho_{s,0}} \sim -\frac{1}{2}y \Rightarrow \rho_-^i = \rho_{s,0} - \frac{1}{4}\rho_c z, \text{ for } \theta = 1 \text{ and } y \ll 1. \quad (45)$$

In words, in the high-salt domain, charge carriers expel 25% of their counterions as salt molecules to a salt solution with the same volume as the suspension. Taking $\theta = 1$, we find on substitution of the salt expulsion from (42) in (31) the osmotic pressure difference:

$$\frac{\Pi - \Pi(y=0)}{2\rho_{s,0}kT} = \frac{y^2}{y+2}, \text{ for } \theta = 1; \quad y = \frac{\rho_c z}{2\rho_{s,0}}. \quad (46)$$

The maximal osmotic pressure difference between a suspension and a solution of equal volume occurs in the low-salt domain:

$$\frac{\Pi - \Pi(y=0)}{2\rho_{s,0}kT} = y, \text{ for } \theta = 1 \text{ and } y \gg 1. \quad (47)$$

One easily verifies that salt addition always lowers the Donnan pressure: the pressure in (46) is always below (47). In the salt-dominated regime, eqn (46) modifies to:

$$\frac{\Pi - \Pi(y=0)}{2\rho_{s,0}kT} = \frac{1}{2}y^2 = \frac{z^2}{8\rho_{s,0}^2} \rho_c^2, \text{ for } \theta = 1 \text{ and } y \ll 1. \quad (48)$$

Also for equal volumes we obtain the quadratic first-order correction to the pressure of uncharged carriers, as could be expected because the quadratic correction is independent of the reservoir size, as was shown in the derivation of eqn (32) in the main text.

References

- 1 E. J. Verwey and J. T. G. Overbeek, *Theory of the Stability of Lyophobic Colloids*, Elsevier, New York, Dover, 1948.
- 2 D. F. Evans and H. Wennerström, *The Colloidal Domain: Where Physics, Chemistry, Biology and Technology Meet*, Wiley-VCH, 1998.
- 3 A. P. Philipse, B. M. W. Kuipers and A. Vrij, *Langmuir*, 2013, **29**, 2859–2870.
- 4 M. Rasa and A. P. Philipse, *Nature*, 2004, **429**, 857.
- 5 P. H. Raven, R. E. Evert and S. E. Eichhorn, *Biology of Plants*, Worth Publishers, 1992.
- 6 W. M. Becker, L. J. Kleinsmith and J. Hardin, *The World of the Cell*, Benjamin/Cummings Publishing Company, San Francisco, 2000.

- 7 B. D. Rose and T. W. Post, *Clinical physiology of Acid–Base and Electrolyte Disorders*, McGraw-Hill, New York, 2001.
- 8 J. B. Tasker, *Bull. Am. Soc. Vet. Clin. Pathol.*, 1975, **4**, 3–13.
- 9 M. Mulder, *Principles of Membrane Technology*, Kluwer, Dordrecht, 1998.
- 10 J. Kucera, *Reverse Osmosis; Design, Processes and Applications for Engineers*, Scrivener Publishing, Salem, 2010.
- 11 J. van Rijssel, R. Costo, A. P. Philipse and B. Ern , in preparation, 2015.
- 12 A. Vrij and R. Tuinier, Structure of Concentrated Colloidal Dispersions, in *Fundamentals of Colloids and Interface Science*, ed. J. Lyklema, Elsevier, 2005.
- 13 A. P. Philipse and A. Vrij, *J. Phys.: Condens. Matter*, 2011, **23**, 194106.
- 14 A. P. Philipse and G. H. Koenderink, *Adv. Colloid Interface Sci.*, 2003, **100–102**, 613–639.
- 15 A. Grattoni, G. Canavese, F. Montecchi and M. Ferrari, *Anal. Chem.*, 2008, **80**, 2617–2622.
- 16 See for example the OSMOMAT 090 Membrane Osmometer, GONOTEC GmbH, Berlin, <http://www.gonotec.com>.
- 17 B. Luigjes, D. M. E. Thies-Weesie, A. P. Philipse and B. Erne, *J. Phys.: Condens. Matter*, 2012, **24**, 245103.
- 18 B. Luigjes, D. M. E. Thies-Weesie, B. Erne and A. P. Philipse, *J. Phys.: Condens. Matter*, 2012, **24**, 245104.
- 19 M. Rasa, B. H. Ern , B. Zoetekouw, R. van Roij and A. P. Philipse, *J. Phys.: Condens. Matter*, 2005, **17**, 2293.
- 20 K. Denbigh, *The Principles of Chemical Thermodynamics*, Cambridge UP, 1959.
- 21 R. J. Hunter, *Zetapotential in Colloid Science*, Academic Press, New York, 1981.
- 22 R. J. Kortschot, J. Lyklema, A. P. Philipse and B. Erne, *J. Colloid Interface Sci.*, 2014, **422**, 65.
- 23 S. Edgecombe, S. Schneider and P. Linse, *Macromolecules*, 2004, **37**, 10089.
- 24 J. van Rijssel, V. F. D. Peters, J. D. Meeldijk, R. J. Kortschot, R. J. A. van Dijk-Moes, A. V. Petukhov, B. H. Erne and A. P. Philipse, *J. Phys. Chem. B*, 2014, **118**, 11000.